Quantum spill-out in few-nanometer metal gaps

Effect on gap plasmons and reflectance from ultrasharp groove arrays in silver

Skjølstrup, Enok Johannes Haahr; Søndergaard, Thomas; Pedersen, Thomas Garm

Published in:
Nanophotonics VII

DOI (link to publication from Publisher):
10.1117/12.2306750

Publication date:
2018

Document Version
Publisher's PDF, also known as Version of record

PROCEEDINGS OF SPIE

SPIEDigitalLibrary.org/conference-proceedings-of-spie

Quantum spill-out in few-nanometer metal gaps: Effect on gap plasmons and reflectance from ultrasharp groove arrays in silver

Enok J. H. Skjølstrup, Thomas Søndergaard, Thomas G. Pedersen

Enok J. H. Skjølstrup, Thomas Søndergaard, Thomas G. Pedersen, "Quantum spill-out in few-nanometer metal gaps: Effect on gap plasmons and reflectance from ultrasharp groove arrays in silver," Proc. SPIE 10672, Nanophotonics VII, 1067205 (4 May 2018); doi: 10.1117/12.2306750

SPIE.

Event: SPIE Photonics Europe, 2018, Strasbourg, France

Quantum spill-out in few-nanometer metal gaps: Effect on gap plasmons and reflectance from ultrasharp groove arrays in silver

Enok J.H Skjølstrup[a], Thomas Søndergaard[a], and Thomas G. Pedersen[a]

[a]Department of Materials and Production, Aalborg University, Skjernvej 4A, DK-9220 Aalborg East, Denmark

ABSTRACT

A gap plasmon is an electromagnetic wave propagating in a gap between two noble metal surfaces. Such gap plasmons have previously been studied using only a classical description of the noble metals, but this model fails and shows unphysical behavior for sub-nanometer gaps. To overcome this problem quantum spill-out is included in this paper by applying Density-Functional Theory (DFT), such that the electron density is smooth across the interfaces between metal and air. The mode index of a gap plasmon propagating in the gap between the two metal surfaces is calculated from the smooth electron density, and in the limit of vanishing gap width the mode index is found to converge properly to the refractive index of bulk metal. When neglecting quantum spill out in this limit the mode index shows unphysical behavior and diverges instead.
The mode index is applied to calculate the reflectance of an ultrasharp groove array in silver, as gaps of a few nm are found in the bottom of such grooves. At these positions the gap plasmon field is highly delocalized implying that it mostly exists in the bulk silver region where absorption takes place. Surprisingly, when the bottom width is a few nm and the effect of spill out at a first glance seems to be negligible, strong absorption is found to take place 1-2 Å from the groove walls as a consequence of the dielectric function being almost zero at these positions. Hence quantum spill out is found to significantly lower the reflectance of such groove arrays in silver.

Keywords: gap plasmons, mode index, electron spill-out, density functional theory, ultrasharp grooves, metal optics.

1. INTRODUCTION

Surface plasmon polaritons (SPPs) are electromagnetic waves bound to and propagating along an interface between a metal and a dielectric.[1] Structures that support such SPPs are called plasmonic structures, and as they are efficient in absorbing incident light,[2,3] and capable to squeeze light below the diffraction limit,[4–7] they have attracted much attention in many research areas, as they also hold applications within solar cells, lasers, and chemical and biological sensors.[8–11] Structures with a small gap of a dielectric material sandwiched between two metal surfaces support gap plasmons, which are electromagnetic waves confined to and propagating along the gap. Refs. 4, 12 studied such gap plasmons localized in gaps of nanometer size between spherical and triangular nanoparticles, while in Refs. 13–16 the gap plasmons were propagating in wider gaps between two parallel metal surfaces, and in Refs. 17–19 they were propagating in rectangular or tapered grooves. In all these papers, the dielectric function takes one value in the gap region and another value in the metal, thus changing abruptly at the interfaces and thereby neglecting quantum spill-out.

In a recent paper studying gap plasmons in few-nanometer gaps in gold when assuming local response,[20] quantum spill-out was taken into account, such that the electron density is smooth, and not a step function, across the interfaces between the metal and the gap. This implies that in the limit of vanishing gap width the mode index of the propagating gap plasmon converges to the refractive index of bulk gold,[20] instead of unphysically diverging as obtained in classical models neglecting spill-out.[14–18] In addition, it was shown in Ref. 20, that the calculated reflectance from an ultrasharp groove array in gold when taking spill-out into account, is in much better agreement with measured reflectance spectra from Refs. 21 compared to classical models found

Further author information: (Send correspondence to ejs@mp.aau.dk)

Nanophotonics VII, edited by David L. Andrews, Angus J. Bain, Jean-Michel Nunzi, Andreas Ostendorf,
Proc. of SPIE Vol. 10672, 1067205 · © 2018 SPIE · CCC code: 0277-786X/18/$18 · doi: 10.1117/12.2306750

in Refs. 21, 22. Hence the effect of quantum spill-out in gold was found to have a significant impact on the propagation of gap plasmons in few-nanometer gaps.[20]

In this paper, we study the same effect in few-nanometer silver gaps, thus applying the same local response method as in Ref. 20, and showing the same converging behaviour of the mode index for small silver gaps. We apply the measured dielectric constant in silver from Ref. 23, where the corresponding dielectric constant for gold was applied in Ref. 20. In addition, we show in this paper that quantum spill-out significantly increases the plasmonic absorption of light in few-nanometer silver gaps. The impact of spill-out is found to be larger in silver than in gold, which is due to a smaller imaginary part of the dielectric constant in silver than in gold.[23]

2. QUANTUM DIELECTRIC FUNCTION

Quantum mechanics gives rise to the tunnel effect, i.e the possibility that electrons can tunnel through a potential barrier, a transition that is forbidden in classical mechanics. We say that quantum spill-out takes place, and Density-Functional Theory (DFT) within the jellium model, treating the positive ions of the metal as a constant charge density inside the metal, provides an effective model for the spill-out.[24,25] The jellium model implies an inhomogeneous density of free (s, p band) electrons, which consists of an exponential tail into the vacuum region and Friedel oscillations in the metal region.[24–26]

Solving the Kohn-Sham equations[24] self-consistently within the jellium model gives the free electron density in the vicinity of a gap. The Local Density Approximation (LDA)[27] is applied when calculating the exchange and correlation potentials in the Kohn-Sham equations, where the correlation term is computed applying the Perdew-Zunger parametrization.[28] For silver, the applied Wigner-Seitz radius is $r_s = 3.02$ Bohr, while r_s equals 3.01 Bohr in gold,[25] which implies that these two noble metals have almost the same bulk electron concentration and Fermi energy. To calculate the electron density across a gap, a structure consisting of two parallel silver slabs of width d, separated by a gap width w, is considered. In order to give the correct density across the gap, the width of the slabs must be sufficiently wide, such that the effect of the slabs being finite is negligible, which is found to be obtained when $d \geq 2.6$ nm. A standing-wave basis of the form $\sin(j\pi(x/L + 1/2))$ is applied to calculate the density, where the length of the structure L is 8 nm, and $j = 1, 2, \cdots, 200$, where it has been found sufficient to include 200 basis functions when $d = 2.6$ nm, in order for the electron density to converge. An optimization process with Anderson mixing parameter[29] of $\alpha = 0.005$ is applied in order to obtain a self-consistent solution, where the process is said to converge when the difference in Fermi energy between two iterations is below 10^{-7} Ha. Due to almost the same bulk electron concentration in gold and silver, the electron density across a silver gap is almost the same as the density across a corresponding gold gap. The electron density for silver is therefore not shown explicitly in this paper, as it is practically identical to the one in Fig. 1 in Ref. 20.

The optical cross sections of metal clusters and spheres[30–33] and metal nanowires[30,34–36] have in the past decade been studied by applying such a jellium model in DFT calculations. In a similar manner, the model has been applied to calculate the plasmon resonance of semiconductor nanocrystals[37] and of metal dimers.[38,39] Furthermore, electron spill-out and non-local effects were studied in Ref. 40, where it was found that spill-out has a significant impact on the propagation of gap plasmons in narrow gaps in gold, while, importantly, the effect of non-locality is much smaller. In addition, the non-local effects were found in Refs. 41–44 to slightly blueshift the plasmon resonances in different metal nanostructures. Time-dependent DFT (TDDFT) was applied in Ref. 34 to study the optical response of metal nanowires, and the results were compared to results obtained using both local and non-local response, and it was found that by including screening as in Refs. 45–47, the results of all three models become in excellent agreement. The impact of non-local effects in nanostructures is thereby not dramatic, and therefore in this paper, similarly to Refs. 20, 31, 32, 36, 37, we neglect the non-local effects are thereby treat the dielectric function as a local response. The local treatment is in the next section shown to imply that the mode index converges to the refractive index of pure silver, instead of unphysically diverging as obtained in classical models. Hence, a local model seems to be sufficient in order to describe the physics regarding the propagation of gap plasmons in narrow metal gaps once spill-out is taken into account.

Once the electron density has been calculated using DFT (not shown in this paper), it is applied to calculate the dielectric function ε across the structure. This function is described as a local Drude term plus an interband

term describing the response of lower lying d-electrons,[1] where it is assumed that no spill-out takes place for these bound electron. Refs. 45–47 considered a phenomenological thin surface layer with ineffective screening, such that the d-electrons should be located in a region a few Å smaller than the jellium region. This has led to calculated plasmon resonances in nanometer-size clusters of gold, silver, and copper in good agreement with measurements. However, in this paper, similarly to Refs. 20, 40, we say that the d-electrons are located in the jellium region, thus neglecting this thin surface layer.

In bulk silver the plasma frequency is $\omega_{p,\text{bulk}} = \sqrt{n_0 e^2/(m_e \varepsilon_0)}$, which implies that the Drude response is $\varepsilon_{p,\text{bulk}}(\omega) = 1 - \omega_{p,\text{bulk}}^2/(\omega^2 + i\omega\Gamma)$.[1] The interband term from the bound d-electrons is included as in Refs. 20, 40, such that the bulk response sufficiently far from the interfaces equals the measured dielectric constant in bulk silver from Ref. 23. This gives the following dielectric function

$$\varepsilon(\omega, x, w) = 1 - \frac{\omega_p^2(x,w)}{\omega^2 + i\Gamma\omega} + [\varepsilon_{\text{silver}}(\omega) - \varepsilon_{p,\text{bulk}}(\omega)]\,\theta(|x| - w/2). \tag{1}$$

The first two terms in Eq. (1) describe the local Drude response of free electrons, where the position dependent plasma frequency $\omega_p(x,w) = \sqrt{n(x,w)e^2/(m_e\varepsilon_0)}$ depends on the electron density $n(x,w)$ calculated using DFT. The damping term in silver has been set to $\hbar\Gamma = 15$ meV. The last term in Eq. (1) describes the response of the bound electrons as modelled by the Heaviside step function θ. Fig. 1 shows for a wavelength of 775 nm the

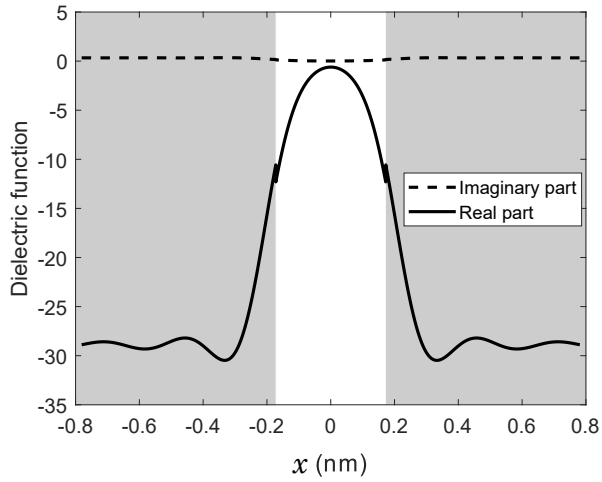

Figure 1. Real and imaginary part of $\varepsilon(x,w)$ for $w = 0.35$ nm, where the wavelength is 775 nm, and the colored areas show the position of the silver surfaces.

dielectric function across a gap of width $w = 0.35$ nm between two silver surfaces, as marked by the colored areas. A jump in its real part at the boundary is clearly seen due to the step function, while the jump in imaginary part is much smaller and hard to see in this figure. The interband term at this wavelength is significantly lower in silver than in gold,[23] why the jump observed in Fig. 1 is much smaller than the corresponding jump in Fig. 2(a) from Ref. 20. The oscillations in the dielectric function found in the silver region are due to the corresponding Friedel oscillations in electron density.

A 3D color plot of the real part of the dielectric function $\varepsilon(x,y)$ in the bottom 25 nm of the ultrasharp groove at a wavelength of 775 nm is seen in Fig. 2(a), where the structure of the groove is shown by the black curve in the xy-plane. The corresponding imaginary part of the dielectric function is shown in Fig. 2(b). In classical models neglecting spill-out[14–18] the imaginary part of the dielectric function is identically zero in the gap region, implying that absorption of light only takes place in the metal. But when spill-out is taken into account, absorption takes place in the entire shown region, as the imaginary part of the dielectric function is non-zero throughout the region.

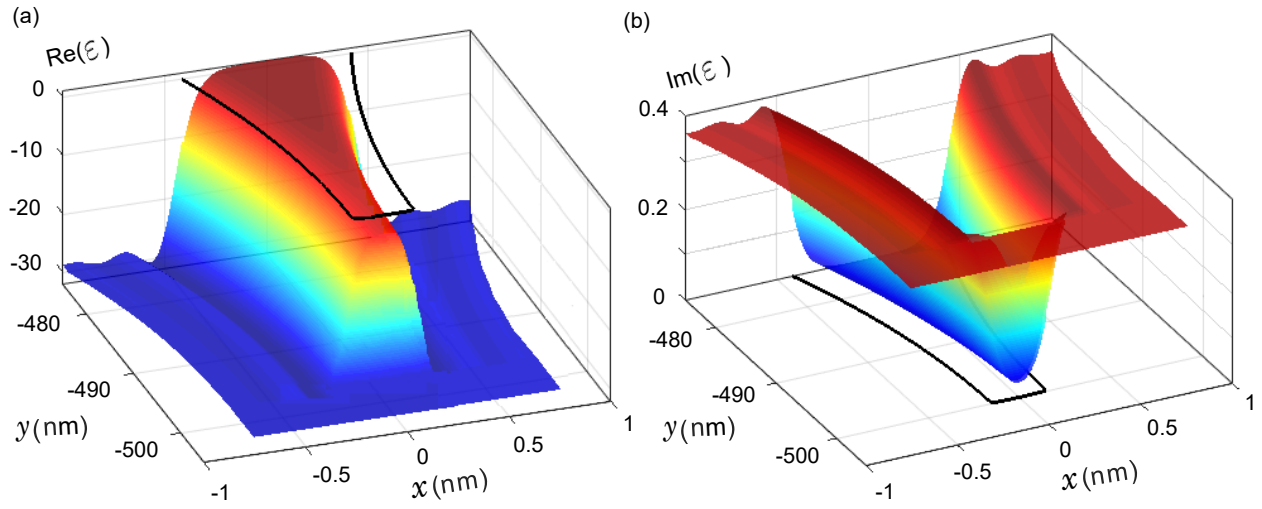

Figure 2. (a) 3D color plot of the real part of $\varepsilon(x, y)$ in the bottom 25 nm of an ultrasharp groove in silver. (b) Corresponding imaginary part of $\varepsilon(x, y)$. The wavelength is 775 nm in both (a) and (b).

Similar figures were shown for gold in Fig. 2(b,c) in Ref. 20 and show the same behaviour as Fig. 2 in this paper, as the shapes of the dielectric functions in gold and silver are roughly the same. In Fig. 2 it is difficult to see the jumps in dielectric function due to the step function, while the jump in real part was clearly observed in Fig. 2(b) in Ref. 20. The imaginary parts look similar in silver and gold, but the scale is very different as silver has a much lower imaginary part of dielectric constant.[23]

Spill-out only significantly affects the dielectric function in Fig.2 at positions close to the interfaces, as the electron density is almost not affected for positions further away. At a first glance, it therefore seems like spill-out only has an effect, when the gap width is below the tunnelling range. But most surprisingly, spill-out has a significant impact on the gap plasmon mode index and plasmonic absorption in few-nanometer gaps, as studied in the next section.

3. MODE INDEX AND ABSORPTION DENSITY OF A PROPAGATING GAP PLASMON

Gap plasmons are p-polarized electromagnetic waves propagating in the y-direction in a gap between two metal surfaces. The associated magnetic field points in the z-direction, and is for a constant w given by[48]

$$\vec{H}(\vec{r}) = \hat{z}H(x, y) = \hat{z}e^{ik_0\beta y}H(x). \tag{2}$$

In Eq. (2) β describes the complex mode index, while $H(x)$ is the transverse field distribution and $k_0 = 2\pi/\lambda$ is the free space wave number. The gap width w has a huge impact on both the mode index and the transverse field distribution as will be shown below.

The top width of the ultrasharp grooves has in agreement with Refs. 20–22 been set to 240 nm, while the shortest considered wavelength is 550 nm. Hence the gap width is smaller than half a wavelength, implying that ordinary waveguide modes can not propagate in the gap.[49] Instead such modes are exponentially damped, and they therefore play a negligible role compared to the much longer propagating plasmonic modes.

A transfer matrix method[50] is applied to calculate the mode index for a fixed gap width w. The x-axis is split into N sufficiently thin layers, where a constant dielectric function is assigned to each layer, where layer thicknesses of $2.7 \cdot 10^{-4}$ nm has been found sufficient in order for the mode index to converge. The magnetic

field to the left and right of the structure is related via the following structure matrix $\mathcal{S}$.

$$\mathcal{S} = \mathcal{T}_{s1} \prod_{i=1}^{N-1} \left(\mathcal{T}_i \mathcal{T}_{i,i+1}\right) \mathcal{T}_N \mathcal{T}_{N,s} := \begin{pmatrix} \mathcal{S}_{11} & \mathcal{S}_{12} \\ \mathcal{S}_{21} & \mathcal{S}_{22} \end{pmatrix}. \tag{3}$$

In Eq. (3) propagation in a particular layer is described by a matrix with a single index, while interfaces are described by a matrix with two indices, and the subscript s denotes bulk silver. Ref. 50 contains expressions for both kinds of matrices in Eq. (3). Left of the structure the magnetic field is then given by

$$\begin{pmatrix} 0 \\ H_L^- \end{pmatrix} = \mathcal{S} \begin{pmatrix} H_R^+ \\ 0 \end{pmatrix}. \tag{4}$$

Here the superscripts + and − denote the direction of light propagation, while the subscripts R and L denote right and left of the structure, respectively, where the boundary conditions are that left (right) of the structure, the light is only propagation in the negative (positive) direction. By combining Eqs. (3) and (4), it is seen that a solution must satisfy that $\mathcal{S}_{11} = 0$. The propagation and interface matrices from Ref. 50 all depend on the mode index β, which implies that $\mathcal{S}_{11}$ is also a function of β. To find the mode index, the same method as in Refs. 20, 48 is applied, where first the values of $\mathcal{S}_{11}$ are evaluated in a region of complex β values. $\mathcal{S}_{11}$ is close to zero in a region if both its real and imaginary parts change sign, and the Newton-Raphson method is hereafter applied to obtain the exact root of $\mathcal{S}_{11}$. As seen in Fig. 1 Friedel oscillations exist in the silver region, and in order for the mode index to converge, it has been found sufficient to include four periods of these oscillations and applying the bulk value beyond this range.

Utilizing the dielectric function from the previous section the mode index of a propagating gap plasmon has been calculated. Fig. 3 shows the mode index as a function of w, where the wavelength is 600 nm in Fig. 3(a) and 775 nm in Fig. 3(b). The mode index when neglecting spill-out (SO) is shown by the blue lines, where the solid

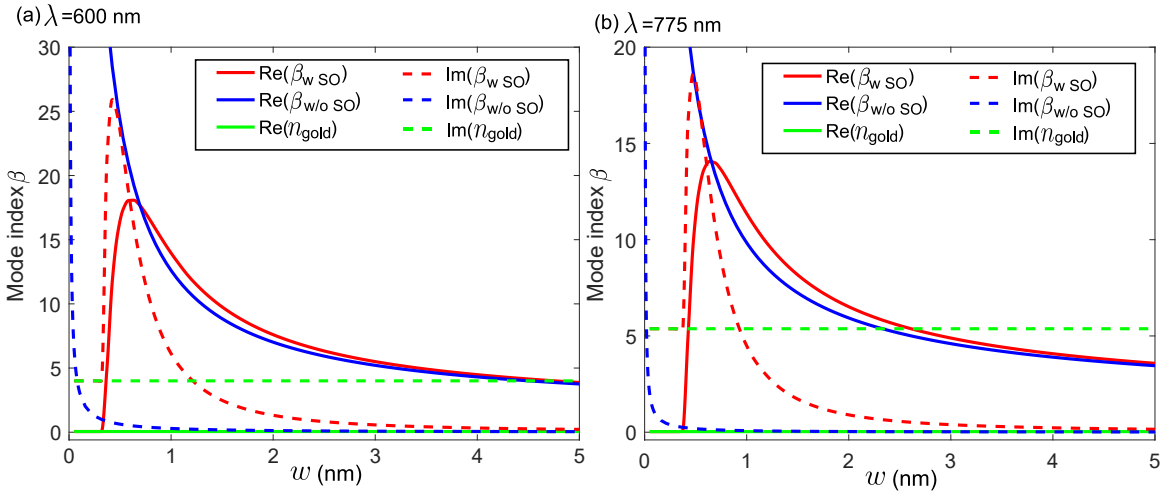

Figure 3. Mode index of a gap plasmon as a function of gap width w. The solid lines shows the real parts, while the dashed lines shows the corresponding imaginary parts. The red lines show the mode index when spill-out (SO) is included, while it is neglected in the results shown by the blue lines. The refractive index of bulk silver from Ref. 23 is shown by the horizontal green lines. The wavelength is 600 nm in (a) and 775 nm in (b).

line shows the real part and the dashed line shows the imaginary part. Here the mode index diverges for small gap widths in agreement with similar studies neglecting spill-out.[14–16] However, a diverging mode index can not be correct from a physical point of view, since in the limit of vanishing gap the structure is simply bulk silver, and the mode index must therefore converge to the refractive index of bulk silver in this limit. This is found to

be the case once spill-out is included, as shown by the red lines in Fig. 3, where again the solid line shows the real part and the dashed line shows the imaginary part. The refractive index of bulk silver from Ref. 23 is shown by the horizontal green lines, where its real part is positive but very small. The mode index when including spill-out converges to the refractive index of bulk silver when the gap width is below 0.35 nm. The dielectric function for $w = 0.35$ nm was shown in Fig. 1 and is quite different from that of pure silver, but nevertheless, when it comes to the mode index of a propagating gap plasmon, the structure behaves almost as pure silver. All the calculated electron densities only depend on the gap width w and the x-coordinate, meaning that in the DFT calculations the structure is considered invariant in both the y- and z-directions. To form the density across the two-dimensional ultrasharp groove, (see Fig. 1 in Ref. 20), the one-dimensional densities are merged together in a region where the curvature of the groove walls is small. As the densities are only one-dimensional, the electron spill-out from the groove bottom is not taken into account. Combining Fig. 1 in Ref. 20 and Fig. 3(a,b) in this paper, it is found that the gap plasmon mode index is almost the same as the refractive index of bulk silver for positions up to 8 nm above the groove bottom. The spill-out from the bottom thus only affects the density in a region where the mode index almost behaves as pure silver, and where no change in mode index is achieved if the dielectric function is slightly modified. This justifies our model neglecting spill-out from the groove bottom. Same result was recently found for gold in Ref. 20. For large gaps, the gap plasmon behaves as an SPP bound to a single interface between silver and air, and the mode index both with and without spill-out converges to the mode index for an infinite gap given by $\sqrt{\epsilon_{\text{silver}}/(\epsilon_{\text{silver}}+1)}$[1] (not shown).

From Fig. 3(a,b) it is seen that when the gap width is a few nm, the real part of the mode index is almost the same with and without spill-out. But the corresponding imaginary part is significantly increased due to spill-out as seen by comparing the red and blue dashed curves. To further illustrate this phenomena, the ratio of the imaginary parts of the mode index with and without spill-out is shown in a color plot in Fig. 4(a). Here

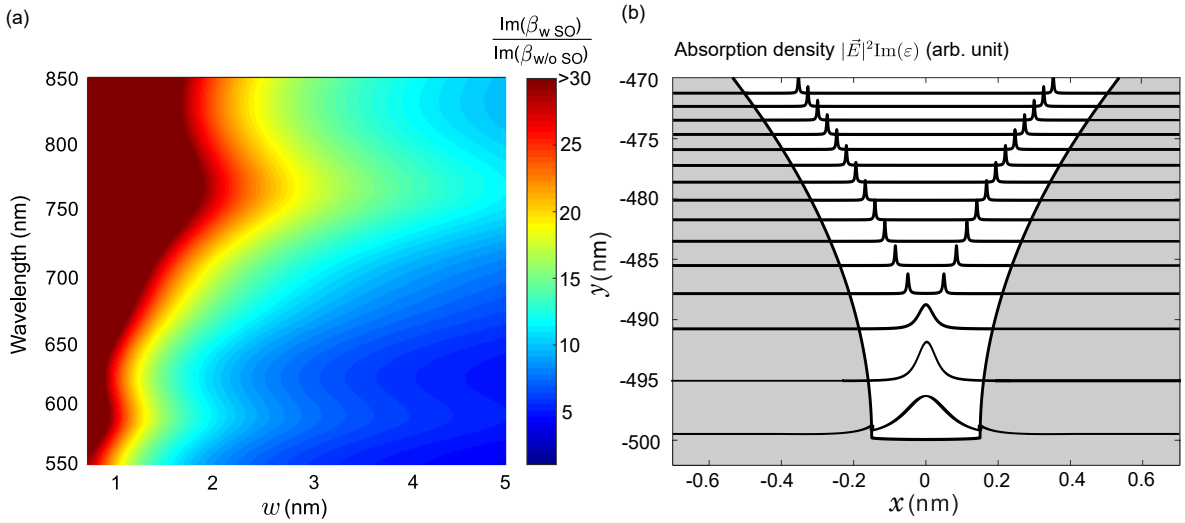

Figure 4. (a) Ratio between imaginary parts of the mode index with and without spill-out (SO). (b) Absorption density in the bottom 30 nm of an ultrasharp groove in silver. Absorption occurs across the entire gap in the bottom 10 nm, while it for longer distances between the groove walls mostly consists of two peaks located 0.15 nm from the interfaces. The wavelength is 775 nm.

it is clearly seen that by including spill-out, the imaginary part of the mode index is remarkably enhanced. In the figure, the color is dark red when the value is above 30, but the maximal value is slightly above 100. Hence, spill-out has a significant impact on the imaginary part of the mode index, even for few-nanometer gaps, where the effect of spill-out at a first glance seems to be negligible as the gap width far exceeds the tunnel regime. A similar result was recently shown for gold in Ref. 20, but there the same ratio was much smaller with a maximum value of roughly 20. Hence in silver, the effect of spill-out has a larger impact on the imaginary part of the mode index than is the case in gold. This is due to the fact that the imaginary part of the dielectric

constant is significantly smaller in silver than in gold.[23]

The imaginary part of the the mode index is associated to the plasmonic absorption, which therefore must be significantly enhanced when spill-out is taken into account. To illustrate this fact, first the electric field $\vec{E}$ is calculated from the magnetic field in Eq. (2) as[1]

$$\vec{E}(x,y) = \frac{i}{\omega\varepsilon_0\varepsilon}\vec{\nabla} \times \hat{z}H(x,y). \tag{5}$$

The electric field is afterwards applied to calculate the absorption density

$$A(x,y) = |\vec{E}(x,y)|^2 \mathrm{Im}(\varepsilon(x,y)). \tag{6}$$

The absorption density in the bottom 30 nm of an ultrasharp groove in silver is shown in Fig. 4(b) at a wavelength of 775 nm. Again the colored area shows the position of the silver. In the bottom 10 nm of the ultrasharp groove, where the distance between the groove walls is below 0.4 nm, absorption takes place across the entire gap. In addition, the absorption density jumps across the interfaces between silver and air in order for the normal component of the displacement field to be conserved.[1] But for positions further above the groove bottom, the distance between the groove walls increases which implies that the absorption density mostly consists of two peaks located 0.15 nm from the interfaces. These peaks are due to the fact that the real part of the dielectric function is zero at these positions, while the imaginary part is small but non-zero, implying that the peaks are finite and not diverging. These peaks are a result of the applied quantum model for the dielectric function, and do not occur in a classical model neglecting spill-out, since in this case absorption can only take place in the metal. It is astonishing that even for gap widths that far exceed the tunnel regime, the effect of spill-out still have a significant impact on the plasmonic absorption. A similar result was recently shown for gold in Ref. 20. How spill-out affects the reflectance from an ultrasharp groove array is examined in the next section.

4. REFLECTANCE FROM AN ULTRASHARP GROOVE ARRAY

The reflecting behaviour of periodic arrays of grooves in gold has been studied in several papers.[19–22,48,51–53] A very low reflectance in a broad wavelength interval can be obtained in ultrasharp grooves in gold,[19–22,48] why such structures are called plasmonic black gold. If the goal instead is to achieve very low reflectance in a narrow wavelength interval the grooves must be rectangular or tapered,[51–53] which can be utilized in thermophotovoltaics.[54–56] Hence the geometrical shape of the grooves decides the reflectance spectrum of the groove arrays. Most papers regarding the optics of groove arrays in metal have neglected spill-out and thereby applied a classical model in the calculations. But recently, spill-out was included in the calculation of the reflectance from an ultrasharp groove array in gold,[20] which led to a reflectance in much better agreement with measurements compared to classical models. In this section, we perform the same calculations for an ultrasharp groove array in silver, utilizing the same stack matrix method as described in Refs. 20, 48. Different kinds of groove arrays in silver have been studied both theoretically and experimentally in Refs. 57–60, but in none of these papers the grooves are ultrasharp and arranged in a 1D periodic array, as is the case for the measurements on gold in Ref. 21. Hence, it is not possible to compare the theoretical reflectance calculated in this paper with any experiments, as was the case in Ref. 20.

The inset in Fig. 5 illustrates the ultrasharp groove array in silver, where the groove height is 500 nm, the top width is 240 nm, and the bottom width is 0.3 nm. Illuminating the array from above gives the reflectances shown by the red and blue lines, where including spill-out results in the reflectance shown by the red line and left y-axis. Neglecting spill-out results in the reflectance shown by the blue curve and right y-axis, and by noticing the very different scale on the two y-axes it is clearly seen that spill-out significantly lowers the reflectance. A similar result was found for gold in Ref. 20, but the difference in reflectance with and without spill-out is larger in silver than in gold, which is due to the fact, that the ratio of imaginary parts of the mode index in Fig. 4(a) is much larger in silver than in gold as mentioned earlier.

Another quantity of the propagating gap plasmons is their transverse field distribution $H(x)$ introduced in Eq. (2). In the following it is therefore investigated which impact spill-out has on this field distribution. For a gap width of 0.45 nm the magnitude of the transverse field $H(x)$ is shown in Fig. 6(a) at a wavelength of 775

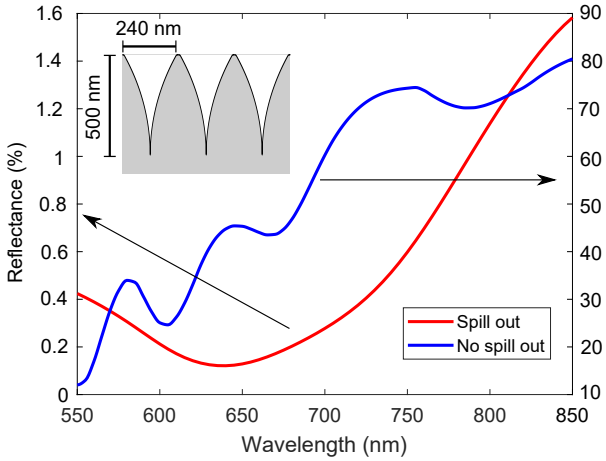

Figure 5. Reflectance for normally incident light from an ultrasharp groove array in silver where the top width of the grooves is 240 nm, the groove height is 500 nm, and the bottom width is 0.3 nm. The red line and left y-axis shows the reflectance when spill-out is included, while the corresponding blue line and right y-axis shows it when spill-out is neglected. The inset shows a schematic of the ultrasharp groove geometry.

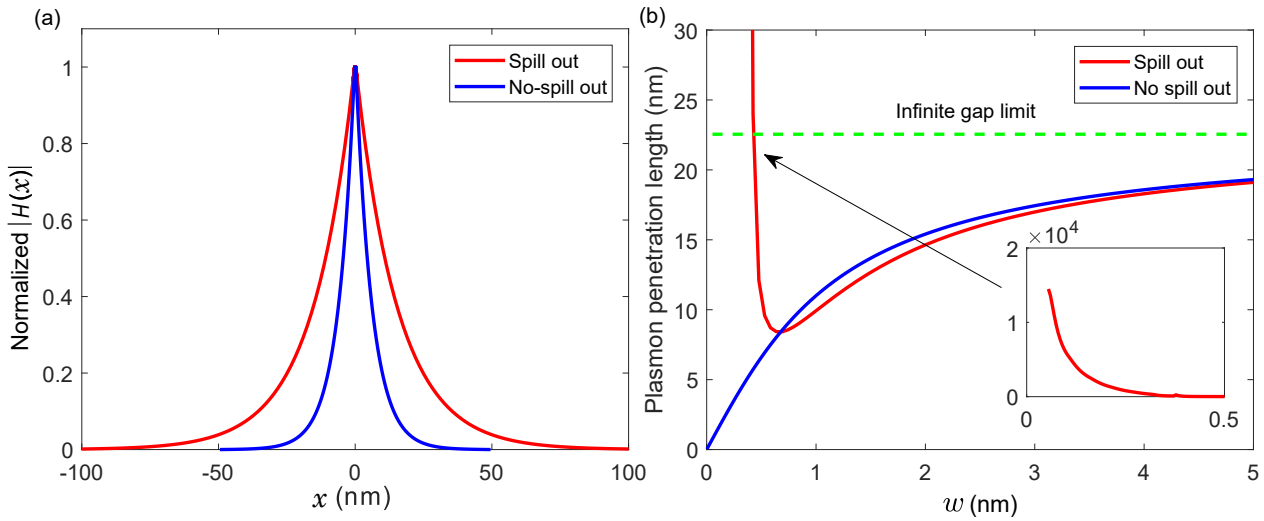

Figure 6. (a) Normalized magnitude of $H(x)$ for a gap plasmon propagating in a gap of width $w = 0.45$ nm. The red line shows the field profile when spill-out is included, while the blue line shows the corresponding field when neglecting spill-out. (b) Corresponding penetration length into the silver as a function of w, where the colors have the same meaning as in (a). The penetration length of a plasmon bound to a single interface between silver and air, i.e in the limit of an infinite gap, is shown by the horizontal green line. The wavelength is 775 nm in both (a) and (b).

nm, where the fields are normalized by their maximal value. Spill-out is neglected for the field shown as the blue line, why the field is partly localized in the gap region. From the blue curves in Fig. 3 the mode index when neglecting spill-out is high, which implies that the imaginary part of $k_x = k_0\sqrt{n_{\text{silver}}^2 - \beta^2}$ is also high. A high value of a reciprocal wave number leads to a field that is localized in real space, and the penetration length into the metal, calculated as $1/\text{Im}(k_x)$,[1] is only 6.0 nm. Including spill-out gives a mode index close to the refractive index of bulk silver, which implies that k_x is very low and the field is therefore more delocalized with a penetration length of 15.8 nm, and most of the field is thereby located in the silver region. But according to Fig. 4(b) the absorption for this gap width mostly consists of two peaks located 0.15 nm from the interfaces,

and not in the bulk silver as is entirely the case when neglecting spill-out. Fig. 6(a) thus shows that when including spill-out the field profile becomes approximately two and a half times broader. This effect becomes more pronounced for smaller w, and for $w = 0.35$ nm the field is almost 100 times broader, which is due to the fact that when including spill-out, the mode index is extremely close to the refractive index of bulk silver.

For other gap widths the same comparison of field profile can be made. The penetration length into the silver is strongly dependent on the gap width, and is shown in Fig. 6(b) at a wavelength of 775 nm. Again spill-out is neglected in the result shown by the blue curve, and for small gaps the field becomes highly localized in the gap with a very short penetration length. The red curve shows the penetration length when spill-out is included and is in the inset of the figure seen to go to infinity for very small gaps, thus in this case the field behaves almost as a plane wave in bulk silver as $k_x \approx 0$. But when the gap width is a few nm the penetration length is almost the same with and without spill-out, as seen by comparing the blue and red lines in the figure. Then it seems like spill-out has no impact on the gap plasmons, but as found in the previous section, the absorption density is significantly enhanced due to spill-out. It is astonishing that even though the penetration length into the metal is almost unaffected by spill-out for few nanometer gaps, the plasmonic absorption is greatly enhanced. The horizontal green line in Fig. 6(b) shows the penetration length of a plasmon bound to a single interface between silver and air, and for large gaps both the red and blue curve converges to this value (not shown).

5. CONCLUSION

In this paper we have applied a quantum mechanical approach and assumed local response in order to describe gap plasmons propagating in few-nanometer silver gaps. When neglecting quantum effects the mode index of the gap plasmons unphysically diverge in the limit of small gaps, but in this paper it is found that quantum spill-out rectifies the divergence, and implies that the mode index converges to the refractive index of bulk silver. Spill-out also has a significant impact on plasmonic absorption in few-nanometer gaps, as strong absorption occurs 1-2 Å from the interfaces. This implies that the reflectance from an ultrasharp groove array is significantly lowered due to spill-out.

Acknowledgement

This work is supported by Villum Kann Rasmussen (VKR) center of excellence QUSCOPE.

REFERENCES

[1] Novotny, L. and Hecht, B., [*Principles of Nano-Optics*], Cambridge, second ed. (2012).

[2] Lalanne, P., Hugonin, J., Liu, H., and Wang, B., "A microscopic view of the electromagnetic properties of sub-λ metallic surfaces," *Surface Science Reports* **69**, 453–469 (2009).

[3] Wang, B. and Lalanne, P., "Surface plasmon polaritons locally excited on the ridges of metallic gratings," *J. Opt. Soc. Am. A* **27**, 1432–1441 (2010).

[4] Marinica, D. C., Zapata, M., Nordlander, P., Kazansky, A. K., Echenique, P. M., Aizpurua, J., and Borisov, A. G., "Active quantum plasmonics," *Sci. Adv.* **1**, 1501095 (2015).

[5] Schuller, J. A., Barnard, E. S., Cai, W., Jun, Y. C., White, J. S., and Brongersma, M. L., "Plasmonics for extreme light concentration and manipulation," *Nat. Mater.* **9**, 193–204 (2010).

[6] Gramotnev, D. K. and Bozhevolnyi, S. I., "Plasmonics beyond the diffraction limit," *Nat. Photonics.* **4**, 83–91 (2010).

[7] Kuttge, M., de Abajo, F., and Polman, A., "How grooves reflect and confine surface plasmon polaritons," *Opt. Express* **17**, 10385–10392 (2009).

[8] Atwater, H. A. and Polman, A., "Plasmonics for improved photovoltaic devices," *Nat. Mater.* **9**, 205–213 (2010).

[9] Berini, P. and Leon, I. D., "Surface plasmon–polariton amplifiers and lasers," *Nat. Photonics* **6**, 16–24 (2012).

[10] Lal, S., Link, S., and Halas, N. J., "Nano-optics from sensing to waveguiding," *Nat. Photonics* **1**, 641–648 (2007).

[11] Anker, J. N., Hall, W. P., Lyandres, O., Shah, N. C., and Duyne, J. Z. R. P. V., "Biosensing with plasmonic nanosensors," *Nat. Mater* **7, 442-453** (2008).
[12] Haberfehlner, G., Schmidt, F.-P., Schaffernak, G., Hörl, A., Trügler, A., Hohenau, A., Hofer, F., Krenn, J., Hohenester, U., and Kothleitner, G., "3d imaging of gap plasmons in vertically coupled nanoparticles by eels tomography," *Nano Lett.* **17**, 6773–6777 (2017).
[13] García-Vidal, F. J., Martin-Moreno, L., Ebbesen, T., and Kuipers, L., "Light passing through subwavelength apertures," *Rev. Mod. Phys.* **82**, 729 (2010).
[14] Søndergaard, T. and Bozhevolnyi, S. I., "Theoretical analysis of plasmonic black gold: periodic arrays of ultra-sharp grooves," *New J. Phys.* **15**, 013034 (2012).
[15] Bozhevolnyi, S. I. and Jung, J., "Scaling for gap plasmon based waveguides," *Opt. Express* **16**, 2676–2684 (2008).
[16] Smith, C. L. C., Stenger, N., Kristensen, A., Mortensen, N. A., and Bozhevolnyi, S. I., "Gap and channeled plasmons in tapered grooves: a review," *Nanoscale* **7**, 9355–9368 (2015).
[17] Bozhevolnyi, S. I., "Effective-index modeling of channel plasmon polaritons," *Opt. Express* **14**, 9467–9476 (2006).
[18] Han, Z. and Bozhevolnyi, S. I., "Radiation guiding with surface plasmon polaritons," *Rep. Prog. Phys.* **76**, 016402 (2013).
[19] Roberts, A., Søndergaard, T., Chirumamilla, M., Pors, A., Beermann, J., Pedersen, K., and Bozhevolnyi., S., "Light extinction and scattering from individual and arrayed high-aspect-ratio trenches in metals," *Phys. Rev. B* **93**, 075413 (2016).
[20] Skjølstrup, E. J. H., Søndergaard, T., and Pedersen, T. G., "Quantum spill-out in few-nanometer metal gaps: Effect on gap plasmons and reflectance from ultrasahrp groove arrays," *Phys. Rev. B.* **97**, 115429 (2018).
[21] Søndergaard, T., Novikov, S., Holmgaard, T., Eriksen, R., Beermann, J., Han, Z., Pedersen, K., and Bozhevolnyi, S., "Plasmonic black gold by adiabatic nanofocusing and absorption of light in ultra-sharp convex grooves," *Nat. Comm.* **3**, 1–6 (2012).
[22] Skjølstrup, E. J. and Søndergaard, T., "Optics of multiple ultrasharp grooves in metal," *J. Opt. Soc. Am. B* **34**, 673–680 (2017).
[23] Johnson, P. and Christy, R., "Optical constants of the noble metals," *Phys. Rev. B* **5**, 4370–4379 (1972).
[24] Lang, N. D. and Kohn, W., "Theory of metal surfaces: Charge density and surface energy," *Phys. Rev. B* **1, 4555-4568** (1970).
[25] Lang, N. D. and Kohn, W., "Theory of metal surfaces: Work function," *Phys. Rev. B* **3, 1215-1223** (1971).
[26] Yan, W., "Hydrodynamic theory for quantum plasmonics: Linear-response dynamics of the inhomogeneous electron gas," *Phys. Rev. B* **91**, 115416 (2015).
[27] Kohanoff, J., [*Electronic structure calculations for solids and molecules - Theory and computational methods*], Cambridge University Press, first ed. (2006).
[28] Perdew, J. P. and Zunger, A., "Self-interaction correction to density-functional approximations for many-electron systems," *Phys. Rev. B* **23**, 5048–5079 (1981).
[29] Eyert, V., "A comparative study on methods for convergence acceleration of iterative vector sequences," *J. Comp. Phys.* **124**, 271–285 (1996).
[30] Yan, W., Wubs, M., and Mortensen, N. A., "Projected dipole model for quantum plasmonics," *Phys. Rev. Lett.* **115**, 137403.
[31] Bakr, O. M., Amendola, V., Aikens, C. M., Wenseleers, W., Li, R., Negro, L. D., Schatz, G. C., and Stellacci, F., "Silver nanoparticles with broad multiband linear optical absorption," *Angew. Chem.* **48**, 5921–5926 (2009).
[32] Zhu, M., Aikens, C. M., Hollander, F. J., Schatz, G. C., and Jin, R., "Correlating the crystal structure of a thiol-protected au25 cluster and optical properties," *J. Am. Chem. Soc.* **130**, 5883–5885 (2008).
[33] Zhang, R., Bursi, L., Cox, J., Cui, Y., Krauter, C., Alabastri, A., Manjavacas, A., Calzolari, A., Corni, S., Molinari, E., Carter, E., de Abajo, F., Zhang, H., and Nordlander, P., "How to identify plasmons from the optical response of nanostructures," *ACS Nano* **11**, 7321–7335 (2017).

[34] Teperik, T. V., Nordlander, P., Aizpurua, J., and Borisov, A. G., "Robust subnanometric plasmon ruler by rescaling of the nonlocal optical response," *Phys. Rev. Lett.* **110**, 263901 (2013).

[35] Stella, L., Zhang, P., García-Vidal, F. J., Rubio, A., and García-Gonzalez, P., "Performance of nonlocal optics when applied to plasmonic nanostructures," *J. Phys. Chem. C* **117**, 8941–8949 (2013).

[36] Marinica, D. C., Kazansky, A. K., Nordlander, P., Aizpurua, J., and Borisov, A. G., "Quantum plasmonics: Nonlinear effects in the field enhancement of a plasmonic nanoparticle dimer," *Nano Lett.* **12**, 1333 (2012).

[37] Zhang, H., Kulkarni, V., Prodan, E., Nordlander, P., and Govorov, A. O., "Theory of quantum plasmon resonances in doped semiconductor nanocrystals," *J. Phys. Chem. C* **118**, 16035–16042.

[38] Maroulis, G., "Comparison of methods for finding saddle points without knowledge of the final states," *J. Chem. Phys.* **121**, 9776 (2004).

[39] Zuloaga, J., Prodan, E., and Nordlander, P., "Quantum description of the plasmon resonances of a nanoparticle dimer," *Nano Lett.* **9**, 987–991 (2009).

[40] David, C. and de Abajo, F., "Surface plasmon dependence on the electron density profile at metal surfaces," *ACS Nano* **8**, 9558–9566 (2014).

[41] Zhu, W., Esteban, R., Borisov, A. G., Baumberg, J. J., Nordlander, P., Lezec, H. J., Aizpurua, J., and Crozier, K. B., "Quantum mechanical effects in plasmonic structures with subnanometre gaps," *Nat. Comm.* **7**, 11495 (2016).

[42] de Abajo, F., "Nonlocal effects in the plasmons of strongly interacting nanoparticles, dimers, and waveguides," *J. Phys. Chem. C* **112**, 17983–17987 (2008).

[43] Raza, S., Toscano, G., Jauho, A., Wubs, M., and Mortensen, N. A., "Unusual resonances in nanoplasmonic structures due to nonlocal response," *Phys. Rev. B* **84**, 121412(R) (2011).

[44] Yan, W., Mortensen, N. A., and Wubs, M., "Green's function surface-integral method for nonlocal response of plasmonic nanowires in arbitrary dielectric environments," *Phys. Rev. B* **88**, 155414 (2013).

[45] Cottancin, E., Celep, G., Lermé, J., Pellarin, M., Huntzinger, J., Vialle, J., and Broyer, M., "Optical properties of noble metal clusters as a function of the size: comparison between experiments and a semiquantal theory," *Theor Chem Acc* **116**, 514–523 (2006).

[46] Kresin, V. V., "Collective resonances in silver clusters: Role of d electrons and the polarization-free surface layer," *Phys. Rev. B* **51**, 1844–1849 (1995).

[47] Liebsch, A., "Surface-plasmon dispersion and size dependence of mie resonance: Silver versus simple metals," *Phys. Rev. B* **48**, 11317–11328 (1993).

[48] Odgaard, M., Laursen, M. G., and Søndergaard, T., "Modeling the reflectivity of plasmonic ultrasharp groove arrays: general direction of light incidence," *J. Opt. Soc. Am. B* **31**, 1853–1860 (2014).

[49] Kong, J. A., [*Electromagnetic wave theory*], John Wiley & Sons, second ed. (1990).

[50] Klein, M. V. and Furtak, T. E., [*Optics*], second ed. (1986).

[51] Skjølstrup, E. J. H., Søndergaard, T., Pedersen, K., and Pedersen, T. G., "Optics of multiple grooves in metal: transition from high scattering to strong absorption," *J. Nanophotonics* **11, 046023** (2017).

[52] Miyazaki, H., Ikeda, K., Kasaya, T., Yamamoto, K., Inoue, Y., Fujimura, K., Kanakugi, T., Okada, M., Hatade, K., and Kitagawa, S., "Thermal emission of two-color polarized infrared waves from integrated plasmon cavities," *Appl. Phys. Lett.* **92**, 141114 (2008).

[53] Greffet, J., Carminati, R., Joulain, K., Mulet, J., Mainguy, S., and Chen, Y., "Coherent emission of light by thermal sources," *Nature* **416**, 61–64 (2002).

[54] Bauer, T., [*Thermophotovoltaics – Basic Principles and Critical Aspects of System Design*], Springer Verlag Berlin, 1st ed. (2011).

[55] Sai, H. and Yugami, H., "Thermophotovoltaic generation with selective radiators based on tungsten surface gratings," *Appl. Phys. Lett.* **85**, 3399–3401 (2004).

[56] Chirumamilla, M., Chirumamilla, A., Yang, Y., Roberts, A. S., Kristensen, P., Chaudhuri, K., Boltasseva, A., Sutherland, D., Bozhevolnyi, S. I., and Pedersen, K., "Large-area ultrabroadband absorber for solar thermophotovoltaics based on 3d titanium nitride nanopillars," *Adv. Opt. Mat.* **5**, 1700552 (2017).

[57] Bora, M., Behymer, E., Dehlinger, D., Britten, J., Larson, C., Chang, A., Munechika, K., Nguyen, H., and Bond, T., "Plasmonic black metals in resonant nanocavities," *Appl. Phys. Lett.* **102**, 251105 (2013).

[58] Søndergaard, T., Bozhevolnyi, S. I., Beermann, J., Novikov, S. M., Devaux, E., and Ebbesen, T. W., "Resonant plasmon nanofocusing by closed tapered gaps," *Nano Lett.* **10**, 291–295 (2010).

[59] Xu, Z., Chen, Y., Gartia, M., Jiang, J., and Liu, G., "Surface plasmon enhanced broadband spectrophotometry on black silver substrates," *Appl. Phys. Lett.* **98**, 241904 (2011).

[60] Takatori, K., Okamoto, T., and Ishibashi, K., "Surface-plasmon-induced ultra-broadband light absorber operating in the visible to infrared range," *Opt. Expr.* **26**, 1342–1350 (2018).